PHYSICAL REVIEW B **81**, 140401(R) (2010)

Ferromagnetism in multiferroic $BiFeO_3$ films: A first-principles-based study

D. Albrecht,[1] S. Lisenkov,[2] Wei Ren,[1] D. Rahmedov,[1] Igor A. Kornev,[3] and L. Bellaiche[1]
[1]*Physics Department, University of Arkansas, Fayetteville, Arkansas 72701, USA*
[2]*Department of Physics, University of South Florida, Tampa, Florida 33620, USA*
[3]*Laboratoire SPMS, UMR 8580 du CNRS, Ecole Centrale Paris, 92295 Chatenay-Malabry, France*
(Received 10 March 2010; published 8 April 2010)

An *ab initio* scheme is developed, and first-principles calculations are performed, to investigate ferromagnetism in $BiFeO_3$ (BFO) *thick* and *ultrathin* films. These systems *all* possess a *weak* magnetization that results from a spin canting (that is induced by the tilting of the oxygen octahedra) and that increases from 0 to $\simeq 0.027\mu_B$ as the temperature is decreased below the Neel temperature. Such findings contradict a suggestion that the coupling between magnetic dipoles and mismatch strain leads to the previously reported large values for the magnetization in BFO films. This spin canting is also found to be essential for the *linear* magnetoelectric effect to occur.

DOI: 10.1103/PhysRevB.81.140401 PACS number(s): 75.70.−i, 75.80.+q, 75.40.Mg

$BiFeO_3$ materials are intensively studied because they possess both a spontaneous polarization and a magnetic ordering, that are *coupled to each other*, at room temperature.[1–24] In BFO *bulks*, the magnetic ordering consists of a cycloidal spin structure.[1,2] On the other hand, the magnetic ordering of BFO *thin films* is a subject of many debates. More precisely, although it is accepted that the cycloidal spin structure is destroyed in BFO films[4] in favor of a spin-canting structure that generates both a magnetization and a *G*-type antiferromagnetic vector, the microscopic origin of such spin canting, as well as, the magnitude of the resulting magnetization are both controversial. For instance, Ref. 5 indicates that such spin canting arises from the so-called Dzyaloshinksy-Moriya interaction[6,7] between magnetic dipoles and *electric polarization* while Ref. 8 states that it is caused by a "mysterious" coupling between magnetic dipoles and the *tilting of the oxygen octahedra*. Similarly, the pioneering experimental work of Ref. 9 reports a high value (around $1\mu_B$) for the magnetization of BFO films while other measurements yield a magnetization being two orders of magnitude smaller.[5,4,10] Some scientists propose that the large value of the magnetization is of *intrinsic* nature[3,9] and is due to the coupling between magnetic dipoles and the strain arising from a lattice-mismatched substrate while others argue that defects are responsible for it.[4,5] Interestingly, even the temperature *behavior* of the magnetization is mostly unknown. In particular, one may wonder if both the ferromagnetic (FM) and antiferromagnetic (AFM) vectors appear at the same temperature, and if they grow in magnitude as the film is cooled below such temperature, or rather if one grows at the extent of the other. Finally, reading the vast literature devoted to BFO systems is quite confusing regarding the requirements for the *linear* magnetoelectric (ME) effect to occur. For instance, Ref. 11 indicates that such linear effect automatically exists once the cycloidal spin structure is destroyed while Ref. 12 did not find a linear ME coefficient in the purely AFM state of BFO. In this Rapid Communication, we use first-principles calculations, as well as, develop an effective Hamiltonian scheme, to address all these important issues.

Let us first determine the real origin of ferromagnetism in BFO systems. For that, we carry state-of-the-art first-principles calculations on ten-atom periodic supercells. These computations are performed within the local spin-density approximation (LSDA)+U technique,[25,26] with the self-consistent value of $U=3.8$ eV.[27] *We also include spin-orbit corrections and noncollinear magnetism*, which are essential to obtain and mimic spin-canting effects.[8] Various space groups within these ten-atom supercells are investigated, namely, rhombohedral $R3m$ and tetragonal $P4mm$ (that only exhibit ferroelectricity); rhombohedral $R\bar{3}c$ and tetragonal $I4/mcm$ (that only possess oxygen octahedra tiltings); and rhombohedral $R3c$ and tetragonal $I4cm$ (that have both ferroelectricity and oxygen octahedra tiltings). We also select different directions of the initial *G*-type antiferromagnetic vector, such as $\langle 001\rangle$, $\langle 110\rangle$, $\langle 112\rangle$, and $\langle 123\rangle$, in these direct first-principles calculations. Our findings are similar to those of Ref. 8, namely, that (i) *no* magnetization occurs if there is no tilting of the oxygen octahedra and (ii) allowing such tilting automatically results in a spin canting, with a weak FM vector (its magnitude is $\simeq 0.027\mu_B$ in the $R3c$ ground state) oriented along the direction generated by the cross product of the AFM vector and the axis about which the oxygen octahedra tilt. Having this in mind, we now develop an effective Hamiltonian scheme for BFO *thick films* (that we simply assume here to correspond to BFO *bulks* with no spin cycloid), for which the total internal energy, E_{tot}, is written as a sum of two terms, $E_{\mathrm{FE-AFD}}(\{\mathbf{u}_i\},\{\eta\},\{\boldsymbol{\omega}_i\})$ and $E_{\mathrm{MAG}}(\{\mathbf{m}_i\},\{\mathbf{u}_i\},\{\eta\},\{\boldsymbol{\omega}_i\})$. $\mathbf{u}_i$ is the local soft mode in unit cell i (which is directly proportional to the electrical dipole centered on that cell) and $\{\eta\}$ is the strain tensor.[28] The $\boldsymbol{\omega}_i$ vector characterizes the oxygen octahedra tilt, or, equivalently, the antiferrodistortive (AFD) motions, in unit cell i. For instance, $\boldsymbol{\omega}_i=0.1(\mathbf{x}+\mathbf{y}+\mathbf{z})$ corresponds to a rotation of the oxygen octahedra by $0.1\sqrt{3}$ radians about [111], when denoting as $\mathbf{x}$, $\mathbf{y}$, and $\mathbf{z}$ the unit vectors along the three $\langle 001\rangle$ pseudocubic directions. $\mathbf{m}_i$ is the magnetic dipole centered on the Fe site i and is assumed to have a fixed magnitude of $4\mu_B$, as consistent with first-principles computations.[14] $E_{\mathrm{FE-AFD}}$ is given in Ref. 29 and involves terms associated with ferroelectricity, strain and AFD motions, and their mutual couplings. E_{MAG} gathers magnetic degrees of freedom and their couplings, and is proposed here to be

$$E_{\mathrm{MAG}}(\{\mathbf{m}_i\},\{\mathbf{u}_i\},\{\eta\},\{\boldsymbol{\omega}_i\}) = \sum_{i,j,\alpha,\gamma} Q_{ij,\alpha\gamma} m_{i,\alpha} m_{j,\gamma} + \sum_{i,j,\alpha,\gamma} D_{ij,\alpha\gamma} m_{i,\alpha} m_{j,\gamma} + \sum_{i,j,\alpha,\gamma,\nu,\delta} E_{ij,\alpha\gamma\nu\delta} m_{i,\alpha} m_{j,\gamma} u_{i,\nu} u_{i,\delta}$$
$$+ \sum_{i,j,\alpha,\gamma,\nu,\delta} F_{ij,\alpha\gamma\nu\delta} m_{i,\alpha} m_{j,\gamma} \omega_{i,\nu} \omega_{i,\delta} + \sum_{i,j,l,\alpha,\gamma} G_{ij,l,\alpha\gamma} \eta_l(i) m_{i,\alpha} m_{j,\gamma} + \sum_{i,l,\alpha,\gamma} B'_{l,\alpha\gamma} \eta_l(i) u_{i,\alpha} u_{i,\gamma} L^2$$
$$+ \sum_{i,j} K_{ij} (\boldsymbol{\omega}_i - \boldsymbol{\omega}_j) \cdot (\mathbf{m}_i \times \mathbf{m}_j), \quad (1)$$

where α, γ, ν, and δ denote Cartesian components. The sums over i run over all the Fe sites while the sums over j run over the first, second and third nearest neighbors of the Fe site i—with the exceptions of the first term where the sum over j runs over *all* the Fe sites and of the last term where the sum over j only runs over the first nearest neighbors of the Fe site i. $\eta_l(i)$ is the lth component (in Voigt notation) of the strain tensor at the site i and L^2 is the square of the magnitude of the G-type antiferromagnetic vector. As in Ref. 12, the first and second term of Eq. (1) represents the dipolar interactions between magnetic moments[28] and exchange interactions, respectively, while the next three terms represent couplings of magnetism with the local soft-modes, AFD degrees of freedom and strain, respectively. The novelties of the present approach with respect to Ref. 12 reside in the introduction of the sixth term (that provides an accurate mimicking of the polarization's behavior in thin films under strain[30]) and the last term of Eq. (1). Note that this last term automatically guarantees that no magnetization exists if the AFM vector lies parallel to the axis about which the oxygen octahedra tilt, as consistent with *ab initio* calculations performed on $BiCrO_3$.[24] The $D_{ij,\alpha\gamma}$, $E_{ij,\alpha\gamma\nu\delta}$, $F_{ij,\alpha\gamma\nu\delta}$ and $G_{ij,l,\alpha\gamma}$ and $B'_{l,\alpha\gamma}$ parameters are extracted from LSDA+U calculations on small supercells.[12,23] K_{ij} is determined to be 2×10^{-6} a.u./(μ_B^2rad) by imposing that the presently developed effective Hamiltonian scheme yields a weak magnetization of $\simeq 0.027\mu_B$ in BFO bulks at low temperature, as predicted by our first-principles computations mentioned above.

Regarding BFO *ultrathin films*, two modifications in their total internal energy are made with respect to $BiFeO_3$ thick films. First of all, the matrices describing the long-range dipolar interactions are replaced by those associated with two-dimensional systems under *open-circuit* (OC) *electrical boundary conditions*.[31] Second, as done for ferroelectric thin films,[32] we add an extra term given by $\frac{1}{2}\lambda\Sigma_i\langle\mathbf{E}_{dep}\rangle\cdot Z^*\mathbf{u_i}$—where $\langle\mathbf{E}_{dep}\rangle$ is the depolarizing field associated with ideal OC conditions and is self-consistently calculated[31] while Z^* is the Born effective charge associated with the local soft mode.[28] The λ parameter allows for a possible screening of $\langle\mathbf{E}_{dep}\rangle$: $\lambda=0$ corresponds to ideal OC conditions while an increase in λ lowers the magnitude of the depolarizing field and $\lambda=1$ corresponds to ideal short-circuit conditions for which this field has vanished. Mechanical boundary conditions associated with *epitaxial* ultrathin films can also be mimicked by freezing some components of the strain tensor.[33,34] On the other hand, *stress-free* films are simulated by allowing the relaxation of *all* the components of the strain tensor. The total energies of BFO films are used in Monte Carlo (MC) simulations with up to 400 000 MC sweeps to obtain finite-temperature properties.

Figures 1(a) and 1(b) display the temperature evolution of the magnitude of the G-type AFM vector, $|\mathbf{L}|$, and of the FM vector, $|\mathbf{M}|$, respectively, in a BFO *thick film*—as modeled by a $14\times14\times14$ periodic supercell and when using the proposed effective Hamiltonian. Two different kinds of simulations are performed: one for which the K_{ij} parameter of Eq. (1) is turned *on* and another for which that coefficient is turned *off*. Figure 1(a) indicates that turning off or on such parameter has merely no effect on the AFM vector and thus on the Neel temperature T_N—which is predicted to be 640 ± 20 K, in excellent agreement with the measured one

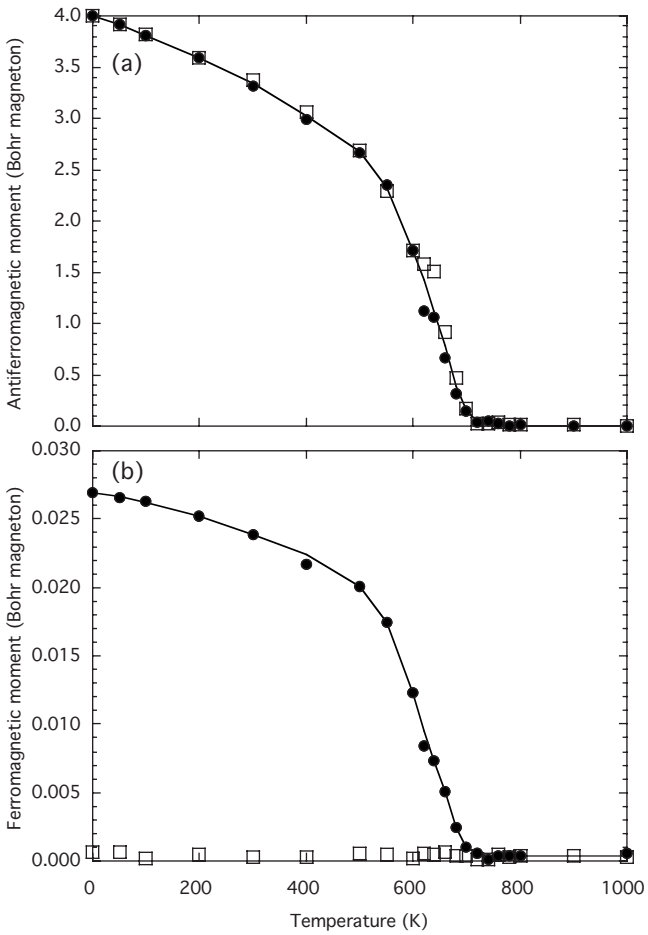

FIG. 1. Magnitude of the AFM vector [Panel (a)] and of the magnetization [Panel (b)] as a function of temperature in a BFO thick film. The filled (respectively, open) symbols correspond to simulations in which the K_{ij} parameter of Eq. (1) has been turned on (respectively, off). Lines are guides for the eyes.

TABLE I. (x,y,z)-Cartesian components of different physical vectors in thick and ultrathin films of BFO at 10 K. **M** and **L** represent the FM and *G*-type AFM vector in μ_B units, respectively. **P** is the polarization and is given in C/m^2. The direction of $\boldsymbol{\omega}$ provides the axis about which the oxygen octahedra tilt while its magnitude yields the angle in radians of such tilts. For instance, such angle is predicted to be 0.237 radians, or, equivalently, 13.6° in BFO thick films, which is in excellent agreement with the value of 13.8° measured in BFO bulks (Ref. 3). Note that the fact that **L** is not exactly found to lie in the (111) plane for thick films is related to the small magnetic anisotropy in and around such plane.

Properties	Thick film	Stress-free ultrathin film	Compressed ultrathin film
M	(0.011,0.011,−0.022)	(0.013,0.011,−0.020)	(0.013,0.011,−0.020)
L	(2.723,−2.877,0.045)	(2.678,−2.944,0.053)	(2.662,−2.959,0.061)
P	(0.404,0.404,0.404)	(0.373,0.373,0.470)	(0.367,0.367,0.479)
$\boldsymbol{\omega}$	(−0.137,−0.137,−0.137)	(−0.127,−0.127,−0.149)	(−0.125,−0.125,−0.151)

≃625–643 K (Refs. 15 and 16) (both simulation also provide a Curie temperature of 1080 ± 20 K, below which the polarization points along [111] and the oxygen octahedra tilt about this [111] direction, as consistent with experiments[15,17,18]). Similarly, no spin cycloid is found when K_{ij} is switched on or off. On the other hand, Fig. 1(b) reveals that turning *on* K_{ij} makes a weak ferromagnetism appearing in BFO thick films at T_N. The AFM and FM vectors *both* increase in magnitude as the temperature is further decreased (when K_{ij} is turned on). The predicted magnitude of this FM vector is around $0.025\mu_B$ at 200 K, which agrees very well with the experimental value $\simeq 0.02\mu_B$ extrapolated down to zero magnetic field in BFO bulk at this temperature.[19,35] Table I further indicates that the FM and AFM vectors both (nearly) lie in a (111) plane and are (nearly) perpendicular to each other in BFO thick films, as consistent with Ref. 8.

Let us now investigate the effect of the spin canting on ME coefficients in BFO thick films. Figure 2 shows the polarization, *P*, as a function of the magnetic field, *B*, applied along the in-plane $[11\bar{2}]$ direction at 20 K. We also performed here the two kinds of simulation described above: one for which no weak ferromagnetism exists (i.e., when $K_{ij}=0$) and another one that exhibits a spin canting (i.e., K_{ij} is switched on). *P* decreases much faster with *B* when the BFO thick film possesses a weak ferromagnetism in its ground state. Such fast decrease is found to originate from the appearance of the *linear* ME effect. As a matter of fact, the data of Fig. 2 can be very well fitted by $P=P_0+\beta B^2$ when no initial weak FM vector exists while they are very well described by $P=P_0+\alpha B+\beta B^2$ when K_{ij} is switched on in Eq. (1)—with $P_0\simeq 0.698$ C/m^2, $\beta=-1.75\pm0.01\times10^{-8}$ $C/T^2\,m^2$, and $\alpha=-8.1\pm0.3\times10^{-7}$ $C/T\,m^2$. In other words, unlike commonly believed,[11] the nonexistence of a cycloidal spin structure does not automatically guarantee the occurrence of the linear ME effect (since none of our simulations yields a spin cycloid). The additional requirement for such linear effect to occur is that a spin-canting-induced ferromagnetism should also exist when no magnetic field is applied. Our simulated β *quadratic* ME coefficient is in remarkable agreement with the magnitude of 1.9×10^{-8} $C/T^2\,m^2$ measured in Ref. 20 and the predicted magnitude of the α *linear* ME coefficient is in-between the experimental value of 4.1×10^{-7} $C/T\,m^2$ (Ref. 21) and the $\simeq13\pm3\times10^{-7}$ $C/T\,m^2$ data from first principles.[24] [Note that α was numerically found to *linearly* increase in magnitude when increasing the K_{ij} parameter from 0 to 5×10^{-6} a.u./(μ_B^2rad), implying that materials having a strong interaction for the last term of Eq. (1) are particularly attractive for yielding a desired enhancement of the linear ME coefficient.]

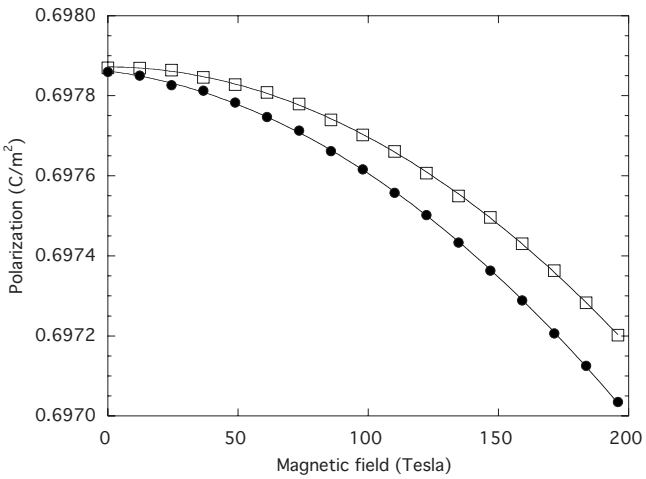

FIG. 2. Polarization as a function of a magnetic field applied along the $[11\bar{2}]$ direction in a BFO thick film at 20 K. The filled (respectively, open) symbols correspond to simulations in which the K_{ij} parameter of Eq. (1) has been turned on (respectively, off).

We now turn our attention to ≃5-nm-thick (001) BFO *ultrathin* films, as modeled by a $12\times12\times12$ supercell that is periodic along the *x* and *y* axes but finite along *z*. The λ screening parameter is chosen to be 0.98 because such value has been found to provide an excellent agreement with experiments in various ferroelectric nanostructures.[36] We consider two different mechanical boundary conditions: the stress-free case vs an epitaxial growth on a $SrTiO_3$ substrate [resulting in a ≃1.5% compressive strain in the (x,y) plane]. Table I reveals that going from a thick film to the stress-free ultrathin film leads to a change in ground state, from a rhombohedral $R3c$ phase—in which the direction of polarization and the axis about which the oxygen octahedra rotate are both along [111]—to a monoclinic Cc state in which the polarization lies along a $[uuv]$ direction with $v>u$ while the tilting of the oxygen octahedra occur about a $[u'u'v']$ direction with $v'>u'$ [note that monoclinic states have indeed

been reported in (001) BFO thin films,[3] which further asserts the accuracy of our scheme]. Such size-induced change in ground state has no significant effect on magnetism. In particular, **M** has a similar magnitude around $0.026-0.027\mu_B$ in both the stress-free thick and ultrathin films at 10 K. Similarly, Table I indicates that (i) both the polarization and the axis about which the oxygen octahedra tilt move further away from [111] when going from the stress-free BFO ultrathin film to the same film but epitaxially grown on a $SrTiO_3$ substrate but (ii) that such change in mechanical boundary conditions does not affect the magnetization (that possesses a magnitude around $0.026\mu_B$). Such predicted weak value is in excellent agreement with the one measured (around $0.02\mu_B$) in some BFO thin films.[4,10] In other words, our calculations fully support the suggestion that the large ferromagnetism ($\simeq 1.0\mu_B$) reported in the pioneering work of Ref. 9 is *not* related to the intrinsic coupling between magnetic dipoles and the mismatch strain.[37]

This work is supported by ONR under Grants No. N00014-04-1-0413, No. N00014-08-1-0915, and No. N00014-07-1-0825, NSF under Grants No. DMR 0701558, No. DMR-0404335, and No. DMR-0080054, and DOE under Grant No. DE-SC0002220. Some computations were made possible thanks to the MRI NSF under Grant No. 0722625 and to a Challenge grant from HPCMO of the U.S. Department of Defense. We thank J. Iniguez, B. Dkhil, B. Dupé, H. Béa, and D. Vanderbilt for useful discussions. S.L. acknowledges the support from the University of South Florida under Grant No. R074021.

[1] I. Sosnowska *et al.*, Physica B **180-181**, 117 (1992).
[2] D. Lebeugle, D. Colson, A. Forget, M. Viret, A. M. Bataille, and A. Gukasov, Phys. Rev. Lett. **100**, 227602 (2008).
[3] L. W. Martin *et al.*, J. Phys.: Condens. Matter **20**, 434220 (2008).
[4] H. Béa *et al.*, Appl. Phys. Lett. **87**, 072508 (2005); H. Bea *et al.*, Philos. Mag. Lett. **87**, 165 (2007).
[5] G. Catalan and J. F. Scott, Adv. Mater. (Weinheim, Ger.) **21**, 2463 (2009).
[6] I. Dzyaloshinsky, J. Phys. Chem. Solids **4**, 241 (1958).
[7] T. Moriya, Phys. Rev. **120**, 91 (1960).
[8] C. Ederer and N. A. Spaldin, Phys. Rev. B **71**, 060401(R) (2005).
[9] J. Wang *et al.*, Science **299**, 1719 (2003).
[10] W. Eerenstein *et al.*, Science **307**, 1203 (2005).
[11] Y. F. Popov *et al.*, JETP Lett. **57**, 69 (1993).
[12] S. Lisenkov, Igor A. Kornev, and L. Bellaiche, Phys. Rev. B **79**, 012101 (2009); **79**, 219902(E) (2009).
[13] I. A. Kornev, S. Lisenkov, R. Haumont, B. Dkhil, and L. Bellaiche, Phys. Rev. Lett. **99**, 227602 (2007).
[14] J. B. Neaton, C. Ederer, U. V. Waghmare, N. A. Spaldin, and K. M. Rabe, Phys. Rev. B **71**, 014113 (2005).
[15] S. V. Kiselev *et al.*, Sov. Phys. Dokl. **7**, 742 (1963); G. A. Smolenskii *et al.*, Sov. Phys. Solid State **2**, 2651 (1961).
[16] P. Fischer *et al.*, J. Phys. C **13**, 1931 (1980).
[17] J. R. Teague, R. Gerson, and W. J. James, Solid State Commun. **8**, 1073 (1970).
[18] R. Haumont, J. Kreisel, P. Bouvier, and F. Hippert, Phys. Rev. B **73**, 132101 (2006).
[19] D. Wardecki *et al.*, J. Phys. Soc. Jpn. **77**, 103709 (2008).
[20] C. Tabares-Munoz *et al.*, Jpn. J. Appl. Phys., Part 1 **24**, 1051 (1985).
[21] J.-P. Rivera and H. Schmid, Ferroelectrics **204**, 23 (1997).
[22] R. Mazumder *et al.*, Appl. Phys. Lett. **91**, 062510 (2007).
[23] S. Lisenkov, D. Rahmedov, and L. Bellaiche, Phys. Rev. Lett. **103**, 047204 (2009).
[24] J. C. Wojdeł and J. Íñiguez, Phys. Rev. Lett. **103**, 267205 (2009).
[25] V. I. Anisimov, F. Aryasetiawan, and A. I. Lichtenstein, J. Phys.: Condens. Matter **9**, 767 (1997).
[26] G. Kresse and J. Hafner, Phys. Rev. B **47**, 558(R) (1993); G. Kresse and J. Furthmüller, *ibid.* **54**, 11169 (1996).
[27] M. Cococcioni and S. de Gironcoli, Phys. Rev. B **71**, 035105 (2005).
[28] W. Zhong, D. Vanderbilt, and K. M. Rabe, Phys. Rev. Lett. **73**, 1861 (1994); Phys. Rev. B **52**, 6301 (1995).
[29] I. A. Kornev, L. Bellaiche, P.-E. Janolin, B. Dkhil, and E. Suard, Phys. Rev. Lett. **97**, 157601 (2006).
[30] A. J. Hatt, N. A. Spaldin, and C. Ederer, Phys. Rev. B **81**, 054109 (2010).
[31] I. Ponomareva, I. I. Naumov, I. Kornev, H. Fu, and L. Bellaiche, Phys. Rev. B **72**, 140102(R) (2005); I. Naumov and H. Fu, arXiv:cond-mat/0505497 (unpublished).
[32] I. Kornev *et al.*, in *Handbook of Advanced Dielectric, Piezoelectric and Ferroelectric Materials: Synthesis, Properties and Applications*, edited by Z.-G. Ye (Taylor & Francis/CRC Press, Boca Raton, FL, 2008), Chap. 19, p. 570.
[33] I. Kornev, H. Fu, and L. Bellaiche, Phys. Rev. Lett. **93**, 196104 (2004).
[34] N. A. Pertsev, V. G. Kukhar, H. Kohlstedt, and R. Waser, Phys. Rev. B **67**, 054107 (2003).
[35] Above 20 Tesla, the cycloidal spin structure of BFO bulk is destroyed in favor of a structure that exhibits a weak magnetization whose magnitude depends on the applied field (Ref. 19).
[36] L. Louis, P. Gemeiner, I. Ponomareva, L. Bellaiche, G. Geneste, W. Ma, N. Setter, and B. Dkhil, Nano Lett., doi:10.1021/n19034708 (2010).
[37] We also performed computations on nanometric BFO dots using a similar effective Hamiltonian and found there a rather weak magnetization too, unlike in Ref. 22 [whose value of $\simeq 0.4\mu_B$ may be due to a large fraction of uncompensated spins from the surfaces (Ref. 5)]. Note that our results cannot rule out the possibility of surface-induced magnetism in BFO nanostructures since such subtle effect is not incorporated in our calculations—mostly because it is likely dependent on the choice of electrodes sandwiching the films or the amount and chemical identity of the absorbants present at the surfaces. However, the fact that our predicted weak magnetization in BFO films is very close to that observed in Refs. 4 and 10 strongly suggests that intrinsic surface-induced magnetism is negligible in BFO nanostructures.